Landsat 8 OLI & TIRS L1T Radiometric Pixel Uncertainty Estimation Update

26 September 2023

Mary Pagnutti

mpagnutti@i2rcorp.com

Innovative Imaging and Research, contractor to the U.S. Geological Survey (USGS)
Earth Resources Observation and Science (EROS) Center, Sioux Falls, SD 57198, USA.
Work performed under USGS Contract 140G0121D0001.

U.S. Department of the Interior
U.S. Geological Survey

L1T Algorithm Overview

- **Algorithm developed to estimate uncertainty for L1 Landsat 8 data**
  - Starts with inherent uncertainty produced for L1R OLI and TIRS data
    - Unevenly spaced grid
  - L1R data is resampled (interpolated) to a regular grid to create L1T product
    - Four components of uncertainty of the resampled L1T product are estimated
      - Propagation of the radiometric noise (L1R) through the interpolation
      - SI traceability (L1R) uncertainty
      - Intrinsic interpolation uncertainty
      - Coupled geometric and radiometric uncertainty
    - The effect of saturated pixels is also considered
  - GUI implementation of uncertainty algorithm has been developed and tested

Relationship to Previous Work

- **Gorrono et. al developed the S-2 Radiometric Uncertainty Tool (RUT)**
  - Emphasized SI traceability based on first principles
  - Produced per-pixel radiometric uncertainty but did not include resampling
- **Developed a similar uncertainty propagation framework for L8 with additional extensions**
  - SI traceability provided by Ball Aerospace
  - Greater emphasis on interpolation related errors
    - Intrinsic interpolation error
    - Sensor noise propagation
    - Coupling of geometric and radiometric uncertainties

[1]*Gorroño, Javier, Ferran Gascon, and Nigel P. Fox. 2015. "Radiometric Uncertainty per Pixel for the Sentinel-2 L1C Products." In Proceedings of SPIE, edited by Roland Meynart, Steven P. Neeck, Haruhisa Shimoda, Toshiyoshi Kimura, 96391G. Toulouse, France. https://doi.org/10.1117/12.2192974.*

Summary of Modifications

- **Improved intrinsic interpolation uncertainty propagation methodology**
  - Original estimate based on a look-up-table approach using a few features
  - Improved algorithm uses analytical approach to directly estimate uncertainty from interpolation equations
- **Level 2A uncertainty product initiated**
  - Extending the Landsat 8 L1 per-pixel uncertainty estimation through L2 processing
    - Sensitivity analysis methods are used to estimate uncertainty for uncorrelated terms
    - Transmission and Rayleigh scattering uncertainty over a range of expected AOT, pressure, angle, water vapor and ozone values will be estimated

Uncertainty Propagation

- **The uncertainty in a quantity y formed by combining N measured quantities x_i through the relationship $y = f(x_1, x_2, \ldots x_N)$ is given by:**

$$u^2(y) = \sum_{i}^{N} \left(\frac{\partial f}{\partial x_i}\right)^2 u^2(x_i) + \sum_{i}^{N} \sum_{j \neq i = 1} \frac{\partial f}{\partial x_i} \frac{\partial f}{\partial x_j} u(x_i, x_j)$$

  - Where: $u(x_i)$ is the uncertainty in x_i and $u(x_i, x_j)$ is the covariance between x_i and x_j. If the combined x_i and x_j are independent (i.e., uncorrelated), the term reduces to zero and the above expression reduces to the "sum of squares" commonly applied.

ISO Guide to the Expression of Uncertainty of Measurement

L1T Uncertainty Components

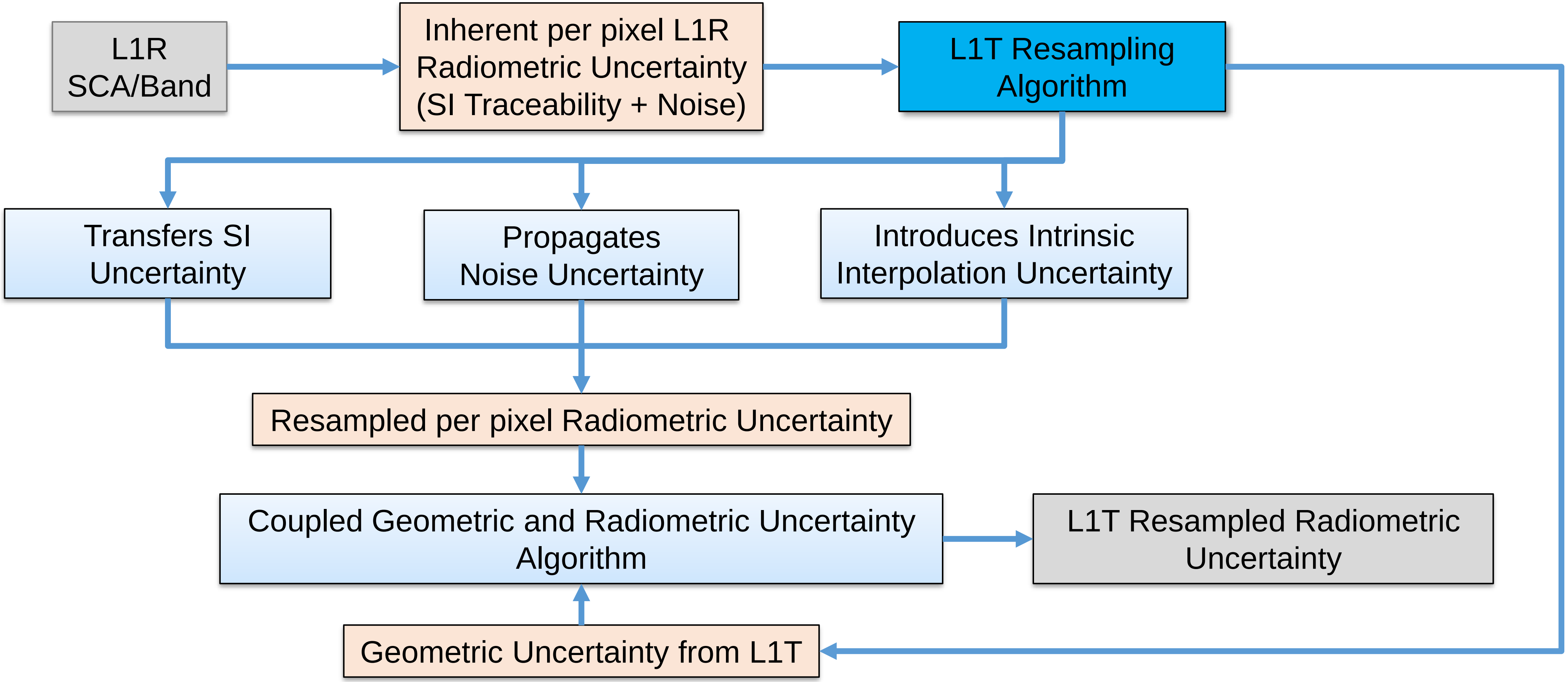

L1T Pixel Uncertainty Estimation Review

Inherent L1R Per Pixel Radiometric Uncertainty

- **OLI L1R radiometric uncertainty combines SI traceable gain uncertainty and radiometric noise model**
  - Ball Aerospace provided pre-launch SI traceable uncertainty values for OLI
    - Uncertainties depend on image radiance (bi-modal)
  - Per-detector radiometric noise model coefficients were developed
    - Validated against published noise model coefficients
- **OLI inherent radiometric uncertainty can be estimated for L1R radiance or reflectance output**
- **TIRS radiometric uncertainty used the same framework as OLI**
    - Noise estimated for every pixel

L1R TOA Radiance Uncertainty (Inherent)

SI Uncertainty + Noise Uncertainty

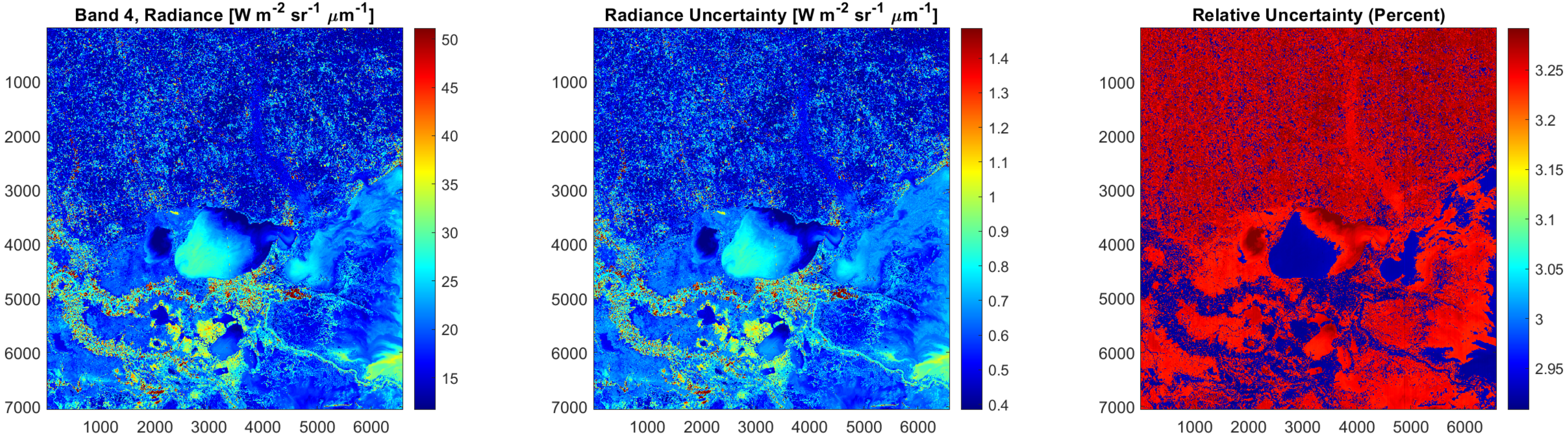

Band 4 $L_{typical}$=22 Wm^{-2}sr^{-1}µm^{-1}

SI Radiance Uncertainty (High)=2.9%
SI Radiance Uncertainty (Low)=3.3%

SI uncertainty dominates throughout the scene

Lake Pontchartrain P22/R39
Red (Band 4) TOA Radiance, Absolute and Relative Uncertainty

L1R TOA Radiance Uncertainty (Inherent)

SI Uncertainty + Noise Uncertainty

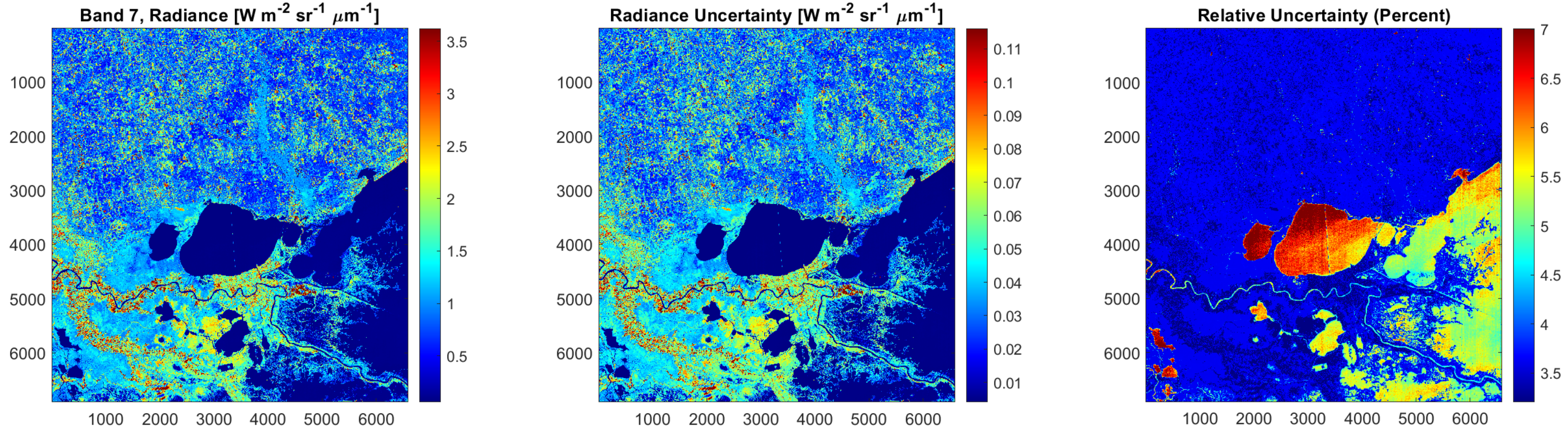

Band 7 $L_{typical}$ radiance = 1.7 $Wm^{-2}sr^{-1}\mu m^{-1}$

SI Radiance Uncertainty (High)=3.2%
SI Radiance Uncertainty (Low)=3.6%

Low signal in SWIR shows increased relative uncertainty due to noise

Lake Pontchartrain P22/R39
SWIR2 (Band 7) TOA Radiance Absolute and Relative Uncertainty

Example TOA Color (RBG) Reflectance Images

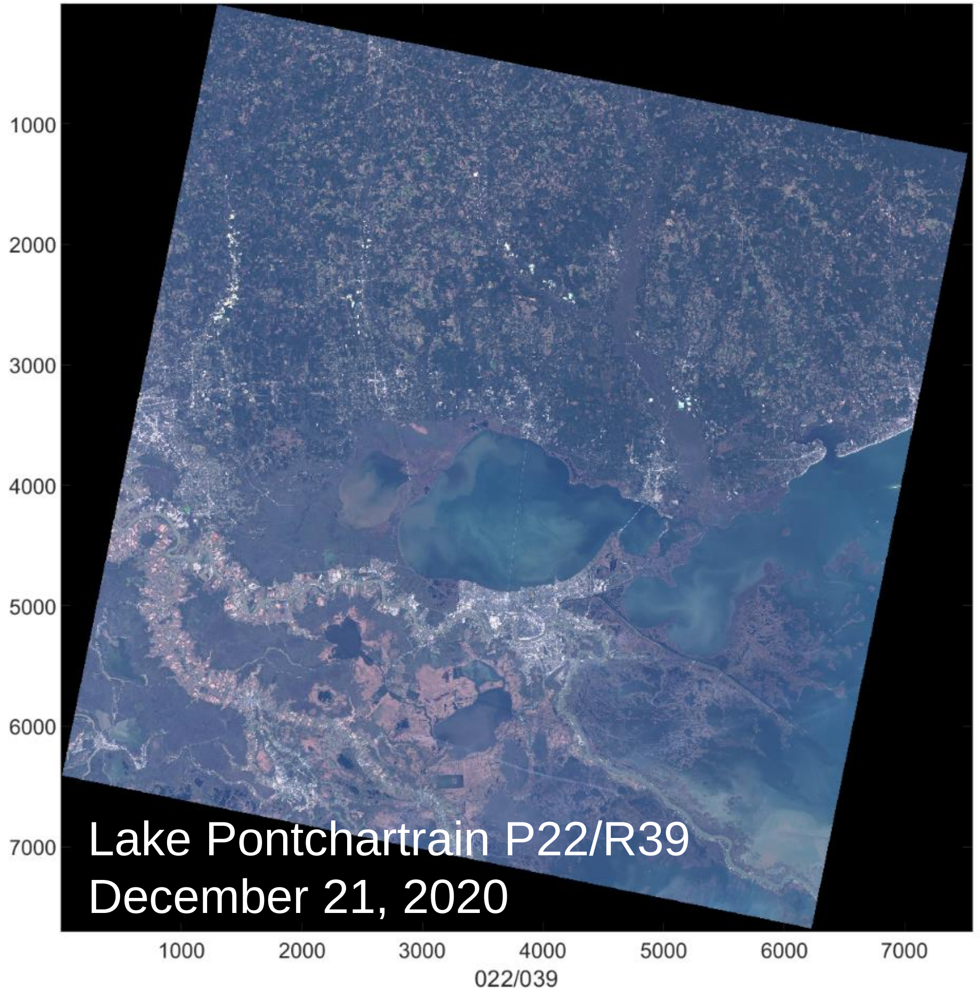

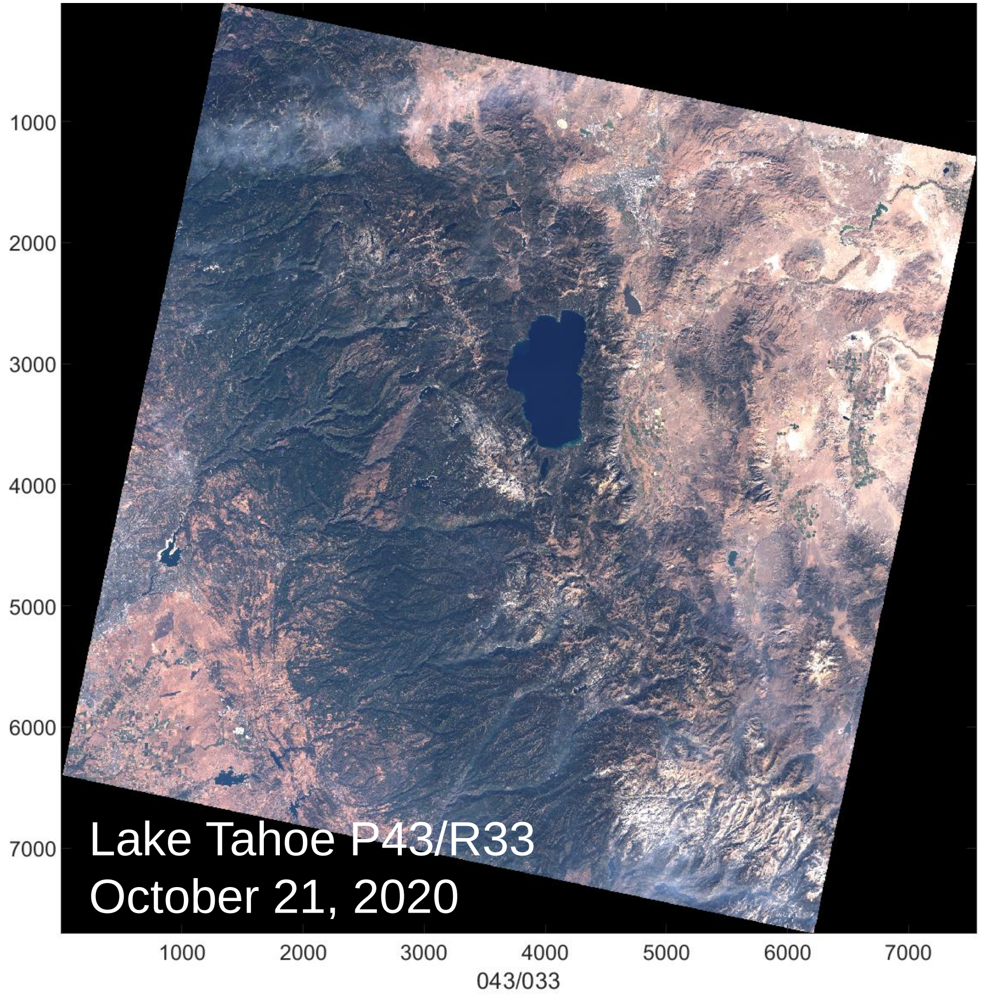

Resampled Radiometric Noise

- **Radiometric noise from the Level 1R data propagates through the interpolation to provide the resampled radiometric noise**
  - Uses the partial derivatives of the interpolator

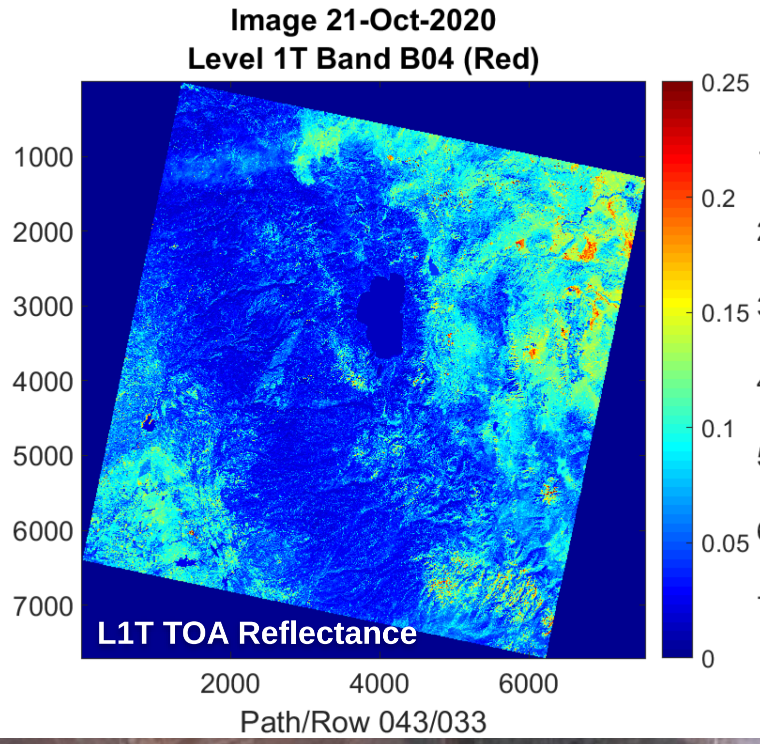

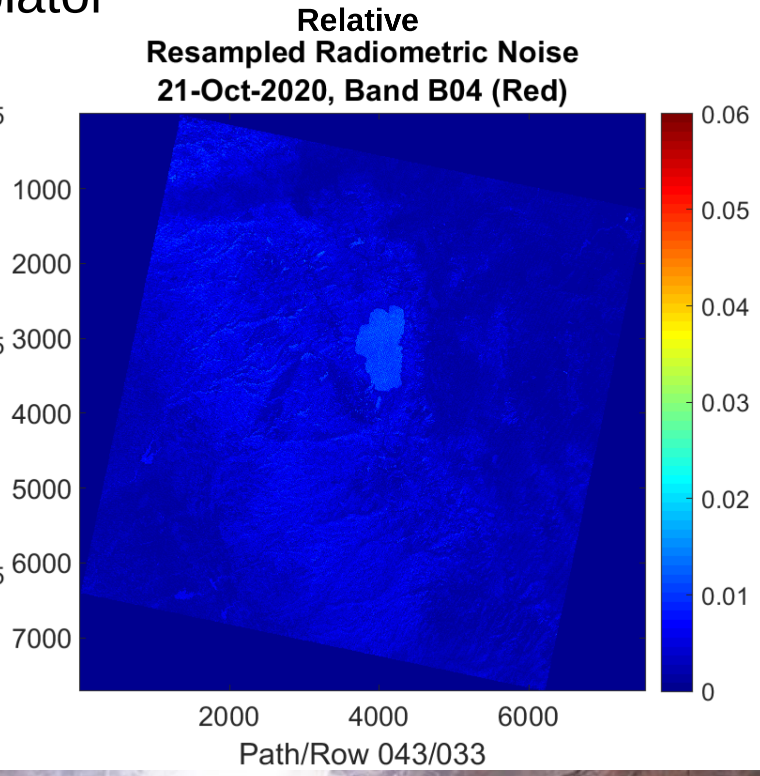

Reflectance Example
The relative resampled radiometric noise in the Lake Tahoe Scene (red band) overall is low, but highest in the lake where the pixels are darkest.

Note: Uncertainty figures shown on same scale to highlight differences in magnitude

SI Uncertainty

- **SI uncertainty is treated separately from the radiometric noise**
  - The SI traceability is not effected by the interpolator

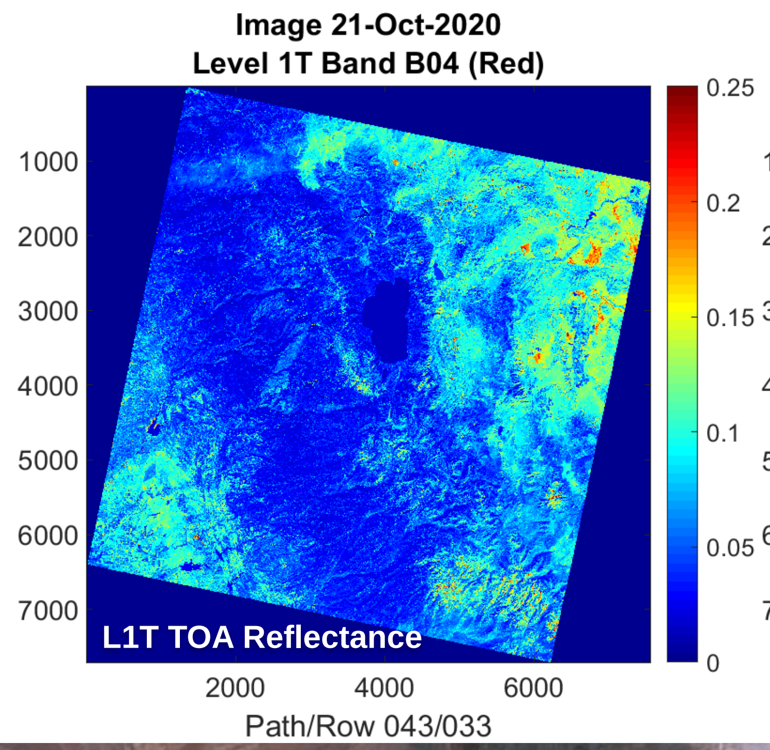

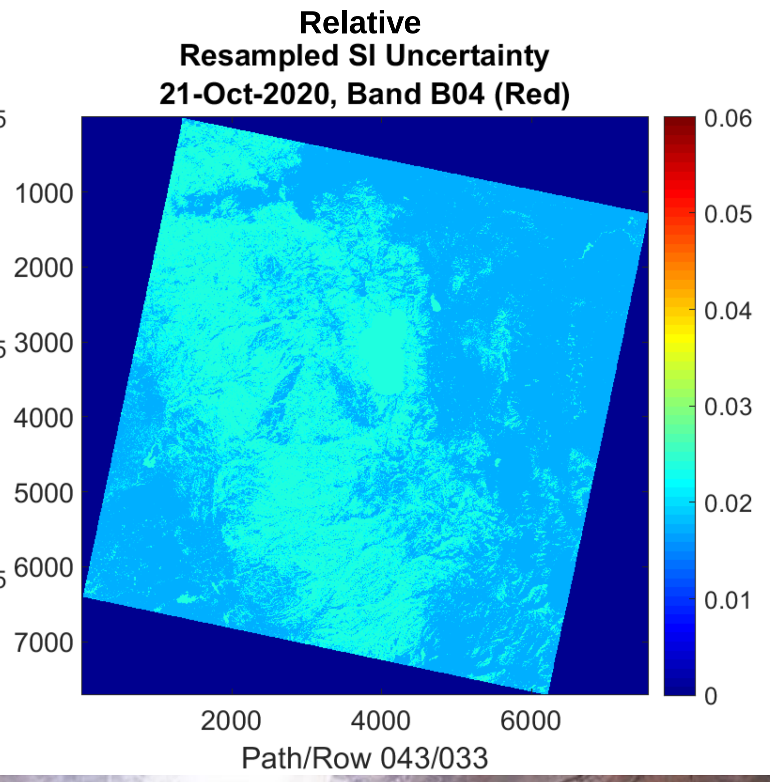

Reflectance Example
The relative resampled SI uncertainty in the Lake Tahoe Scene (red band) is largely bi-modal with some interpolation.

Note: Uncertainty figures shown on same scale to highlight differences in magnitude

Coupled Geometric and Radiometric Uncertainty

Coupled uncertainty of an edge, in one dimension

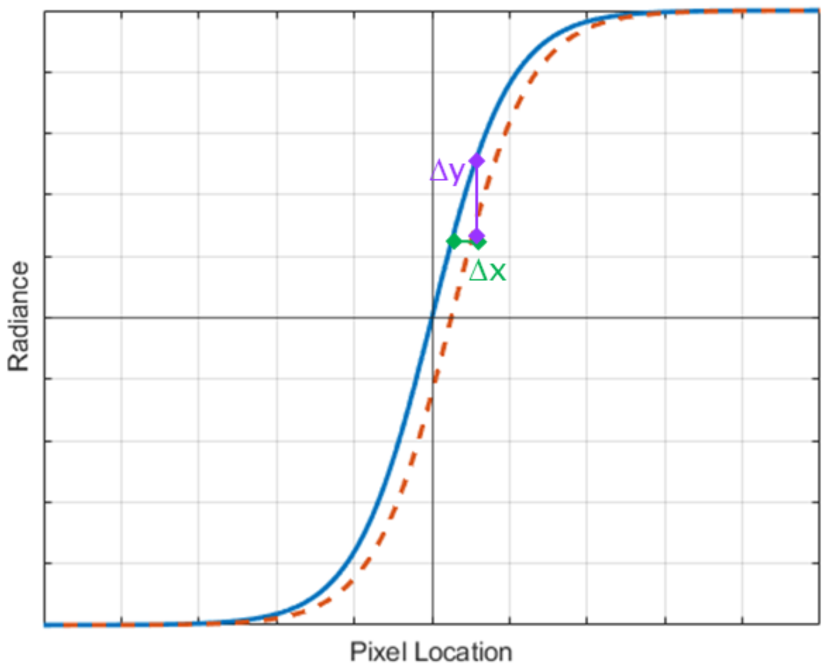

- Two curves represent an edge on the ground imaged on different days
  - Δy is the radiometric uncertainty due to geometric uncertainty (Δx)
- Gradient of the edge = $\frac{\partial y}{\partial x}$
- By generalizing, $\partial y = \frac{\partial y}{\partial x} \partial x$,

  we can estimate coupled geometric and radiometric uncertainty as,

$$\Delta y \approx \frac{\partial y}{\partial x} \Delta x$$

Coupled Geometric and Radiometric Uncertainty

- **Uncertainty in position will affect the result of resampling**
  - How large this effect is depends on the slope of the data at the point of the position error and the amount of uncertainty in position
  - Estimated as the product of the derivative of the image and the positional error

$$u_{cgr,x} = \frac{dImage}{dx}\Delta x$$

$$u_{cgr,y} = \frac{dImage}{dy}\Delta y$$

$$u_{cgr} = \sqrt{u_{cgr,x}^2 + u_{cgr,y}^2}$$

Areas with higher gradients have higher coupled geometric radiometric uncertainty. Easier to see in the relative uncertainty image.

Note: Uncertainty figures generated with same scale to highlight differences in magnitude

Image 21-Oct-2020
Level 1T Band B02 (Blue)

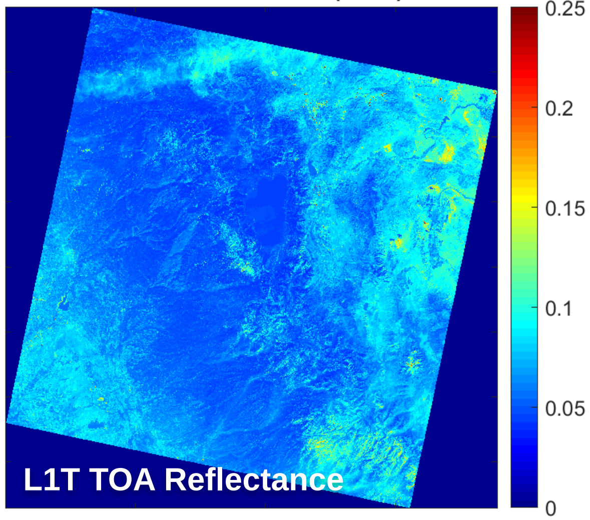

Path/Row 043/033

Absolute Coupled Geom. and Rad. Uncertainty
21-Oct-2020, Band B02 (Blue)

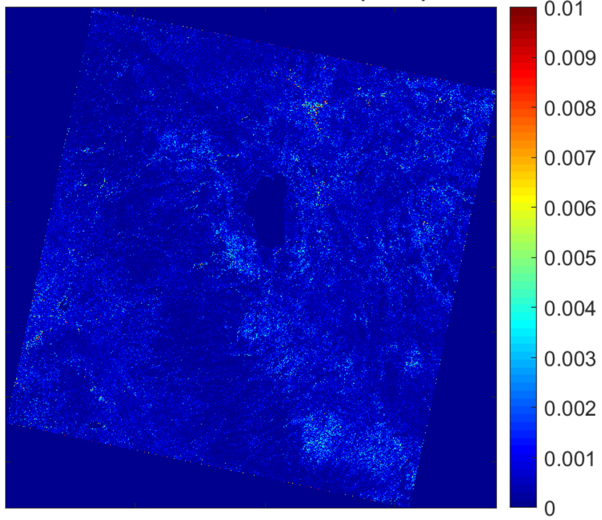

Path/Row 043/033

Relative Coupled Geom. and Rad. Uncertainty
21-Oct-2020, Band B02 (Blue)

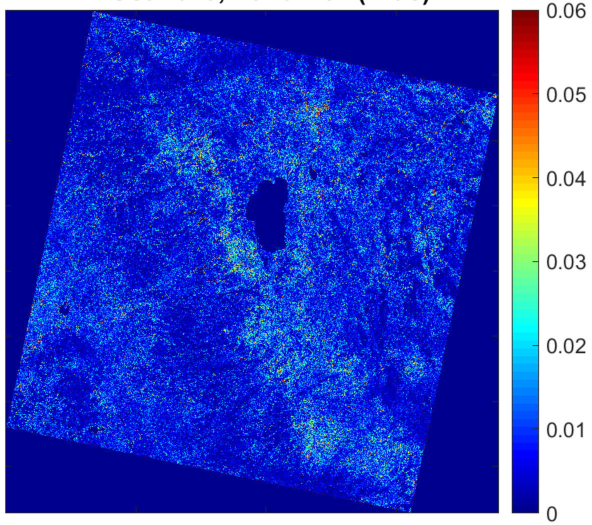

Path/Row 043/033

Saturated Pixels

- **Saturated pixels have unknown uncertainty**
  - The lack of information will propagate through the resampling
    - Output locations that have a saturated input pixel in their resampling kernel will also have unknown uncertainty
  - Pixels affected by saturation assigned an "unknown" uncertainty

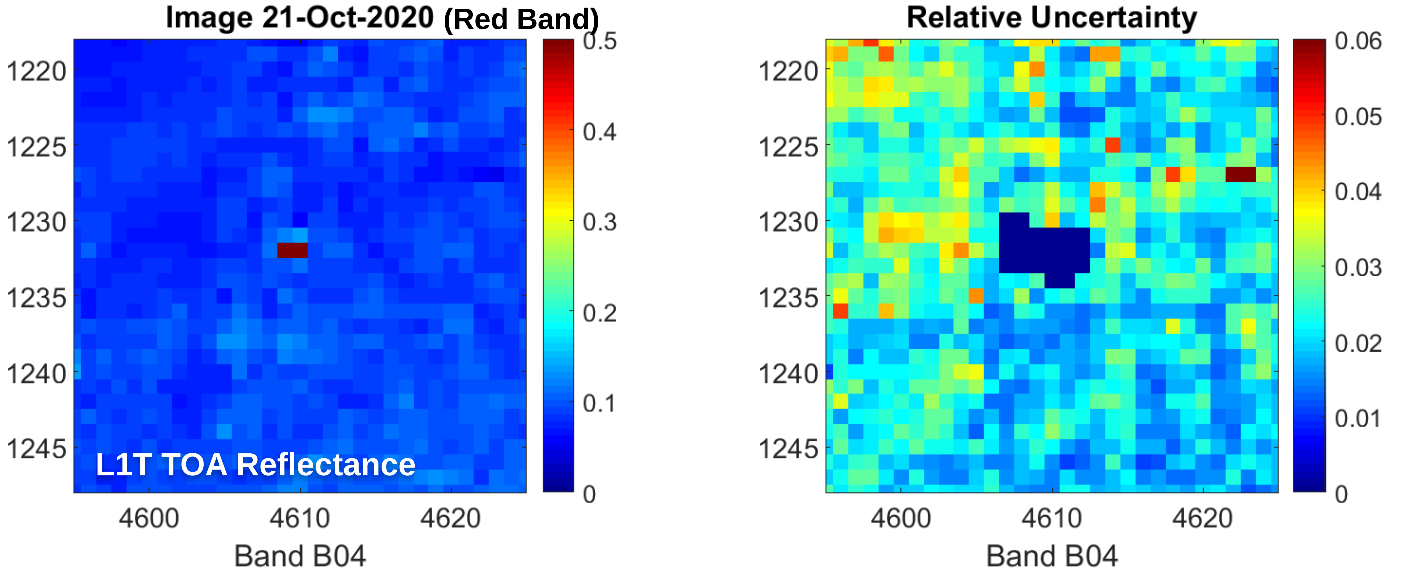

(Left) The red pixels are the result of a single saturated pixel in the original L1R data. (Right) The dark blue area shows the pixels affected by the saturation during interpolation. These have an unknown uncertainty and are masked out (-9999).

Note: Uncertainty figures shown on same scale to highlight differences in magnitude

Improved Intrinsic Interpolation Uncertainty Propagation Methodology

Intrinsic Interpolation Uncertainty

- **Interpolation is used to estimate data values between observation points**
  - The estimate depends on the shape of the underlying function being used in the interpolation
    - There are many different choices for the interpolation functions (linear, cubic, nearest neighbor, spline, etc.)
    - There is some inherent error in the interpolation because the true source data has no connection to the function selected

Intrinsic Interpolation Uncertainty

- **Landsat 8 uses two different interpolation methods to make these estimations**
  - In-track uses cubic convolution interpolation
  - Cross-track uses Akima interpolation

Both of these are cubic polynomial interpolators

- **Lagrange cubic polynomial interpolation has a known error estimate**
  - This interpolator is a cubic polynomial interpolator
  - The error estimate requires determining the 4^{th} derivative of the source
  - Can be extended to other cubic polynomial interpolators

Example Source vs. Interpolator

Cubic Convolution

- The four red x's simulate evenly spaced observations of the L1R sampling in the in-track direction
- The blue curve is the continuous sample
- The black curve is the cubic Lagrange polynomial through the 4 observation points
    - It is well known, and has known error estimate
- The magenta curve is the cubic convolution interpolation
    - Interpolation would only apply to the region of interest, between the vertical dotted black lines

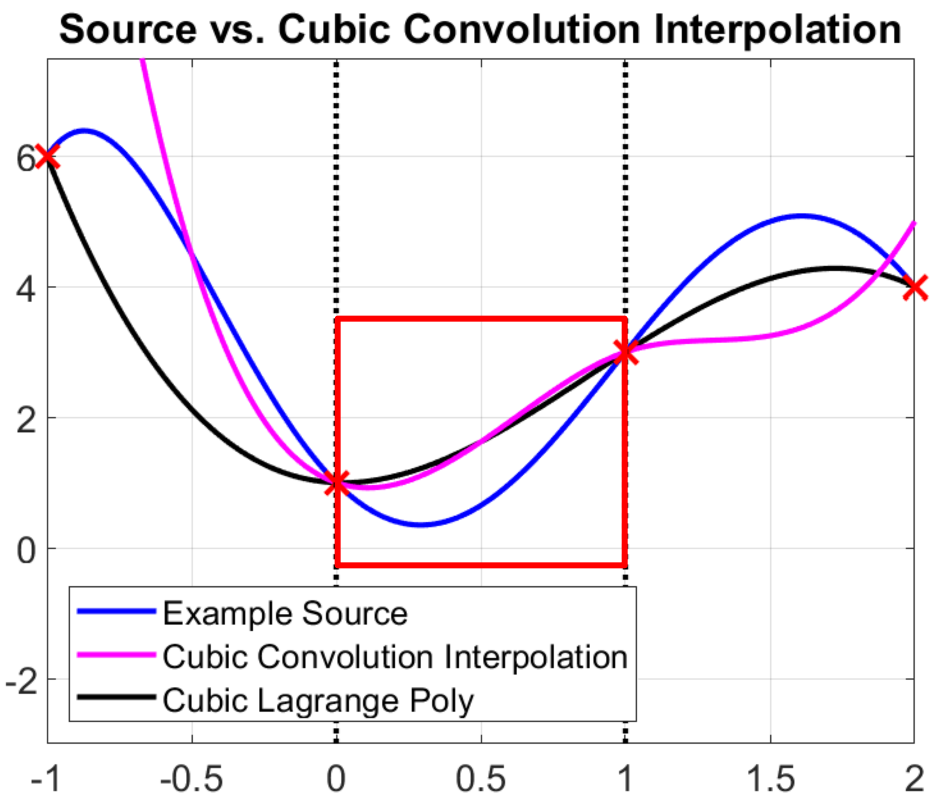

Inside the ROI (between 0 and 1):
- Both cubic polynomials overestimate the source function
- Neither polynomial is better than the other over the whole region
- Lagrange polynomial has known error, and cubic convolution interpolation error, while unknown, can be bounded

Example Normalized Target – Stressing Case

- The black line is a normalized edge
- The blue line is a 1 m oversampling of the edge as it would be seen by Landsat 8
- The four red x's are the observations of the edge at Landsat 8's 30 m resolution
- The red line is the cubic convolution of the four observations over the region of interest

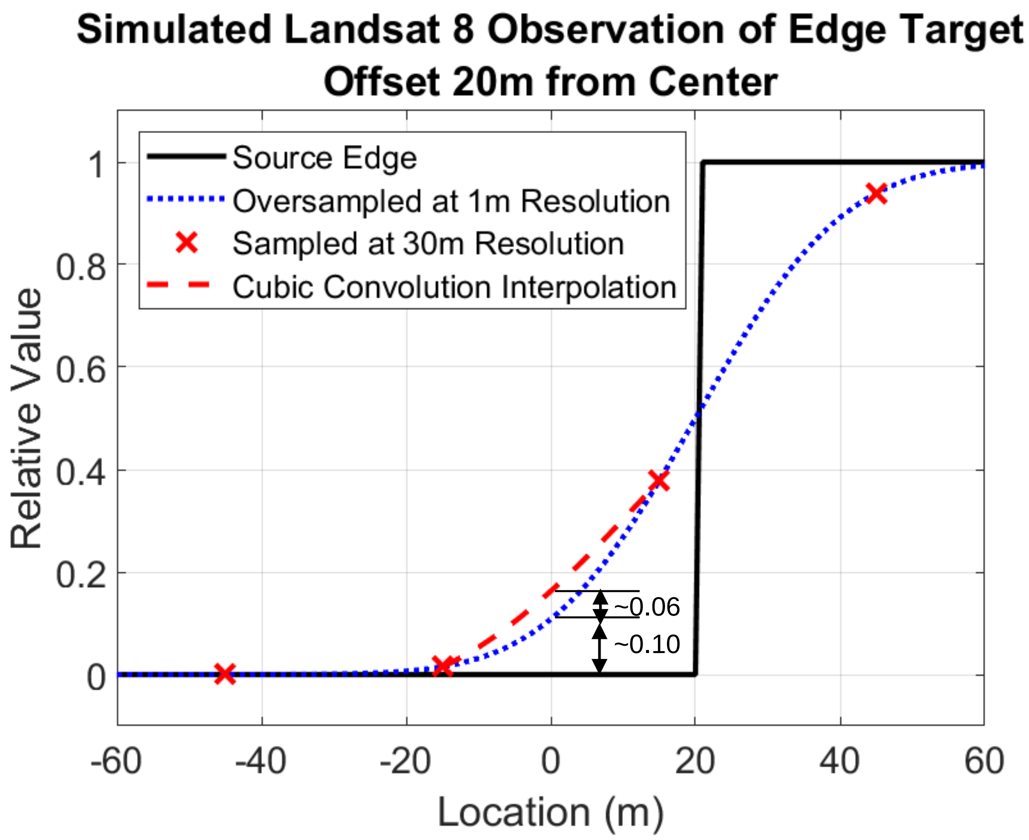

Residuals inside the ROI:

- Interpolator is off by ~0.06 from the actual value of the edge (residual value).
- The normalized edge response is close to 0.1, so this residual value is a significant error

Cubic Convolution vs. Lagrange Polynomial

Example Normalized Edge

- Simulated, oversampled edge
- Dotted black line is the cubic Lagrange polynomial
  - Passes through the 4 observation points
- Dashed red line is the cubic convolution interpolator
  - Extended beyond the region of interest

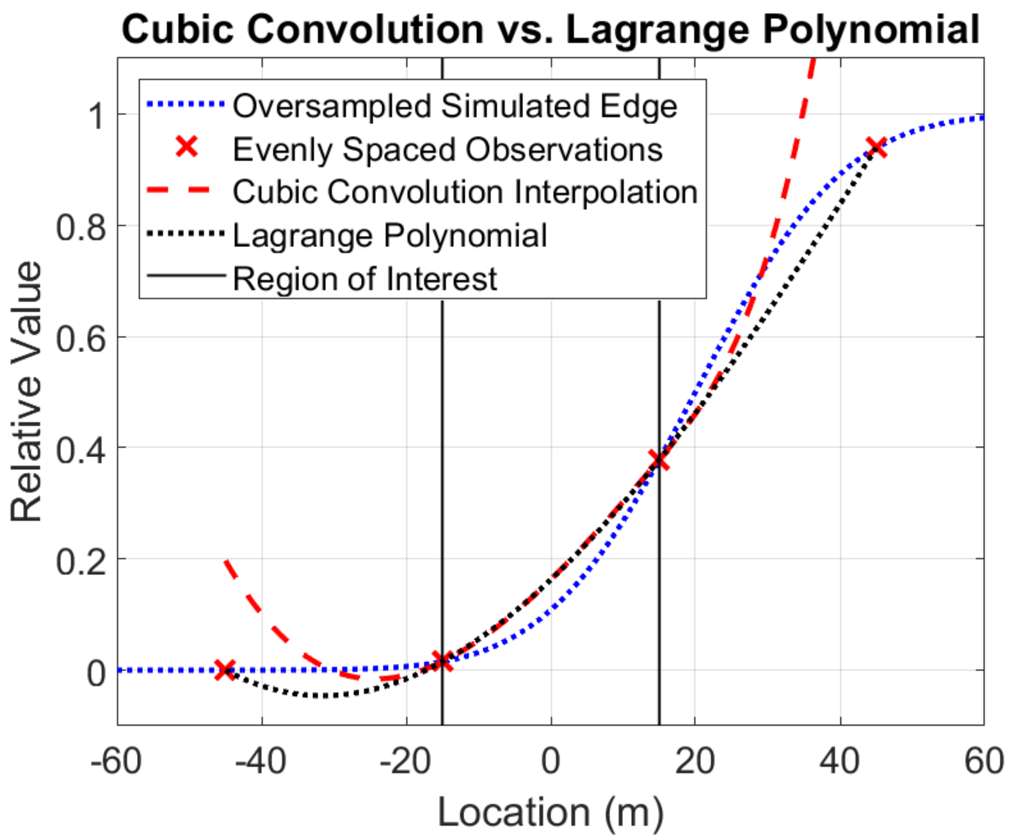

For the normalized edge case:

- Inside the region of interest, the cubic convolution is difficult to distinguish from the cubic Lagrange polynomial
- The cubic Lagrange polynomial line has a known error estimate in terms of the 4th derivative of the observation data.

Intrinsic Interpolation Uncertainty Theoretical Background

- **The error estimate for Lagrange polynomial interpolation is known**
  - Based on the 4th derivative of the source (which is generally not known)
- **This error estimate can be extended to Akima and cubic convolution interpolators**
  - The interpolators used by Landsat 8 are often close to the Lagrange polynomial
    - Cubic convolution polynomial equals the Lagrange polynomial at the center of the region of interest
  - The absolute difference between the Lagrange polynomial and the interpolated value is the same as the absolute difference in their errors as compared to the source
- **The 4th derivative of the source can be estimated from the point spread function (PSF) and the observed values**
- **The combination of these three points gives an upper bound on the reasonable residual error that might be seen for a set for observations**
  - Conservative estimate
  - We assume the distribution of possible sources that give a particular observation is normal (gaussian)
  - This maximum error bound is divided by 5 to estimate the 1-sigma uncertainty
    - More effort is needed to determine the relationship between the maximum and the 1-sigma bound

Intrinsic Interpolation Uncertainty Estimate

Simulated Edge

- Estimate of the intrinsic interpolation uncertainty (red curve).
  - Equation is given below, and explained in more detail in the Appendix.
- Actual residual error (blue curve) between the simulated edge example and the interpolated value at that point in the region of interest (ROI).

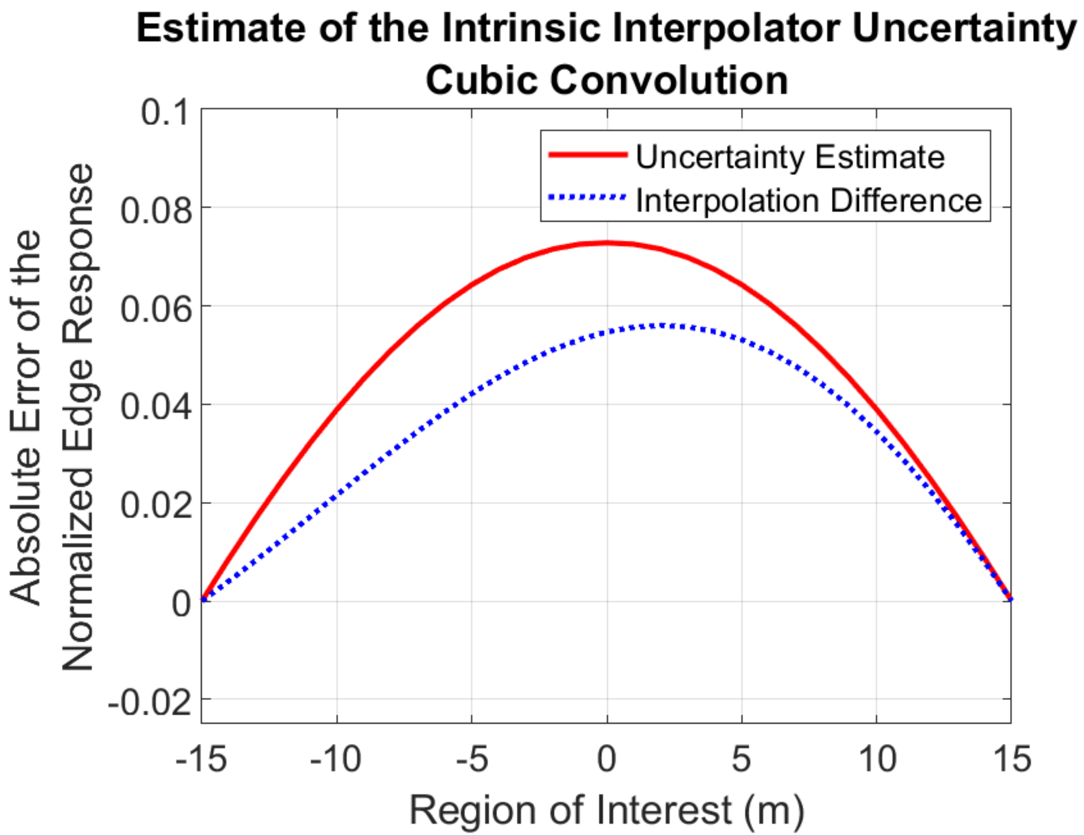

Notes:

- Uncertainty is not a measure of the residuals
- It is an estimate of what the 1-sigma error would be for all possible sources that could result in these 4 observation points.
- This is a stressing case. The uncertainty is close to 0.07, which is a significant error.

$$u_{cc}(x) \approx \frac{1}{5}\left[\left(\frac{\max\limits_{z}\left(\left|f^{(4)}(z)\right|\right)}{4!}\right)\prod_{i=1}^{4}(x - x_i) + \left|p_{L(x)} - p_{cc(x)}\right|\right]$$

The error estimate is a 4th degree polynomial.
A bound for $f^{(4)}$ is established.
The bound on the derivative gives an upper bound on the maximum error that can be expected. For now, this maximum is divided by 5 to estimate the 1-sigma error, with the assumption that 5 standard deviations is near the reasonable limit for normal distributions.

Intrinsic Interpolation Uncertainty - Reflectance

Lake Tahoe P43/R33
Blue (Band 2)

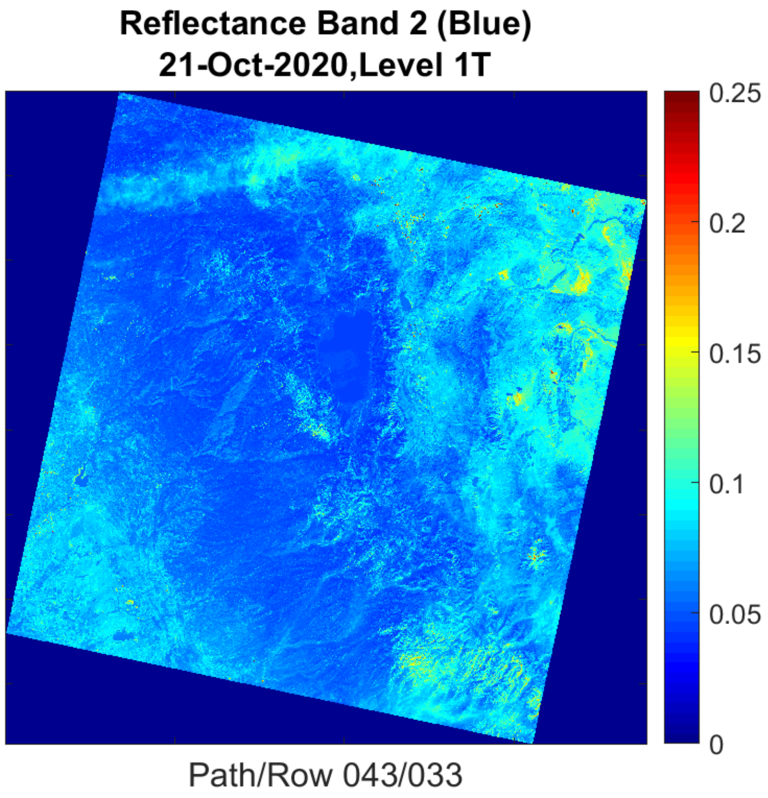

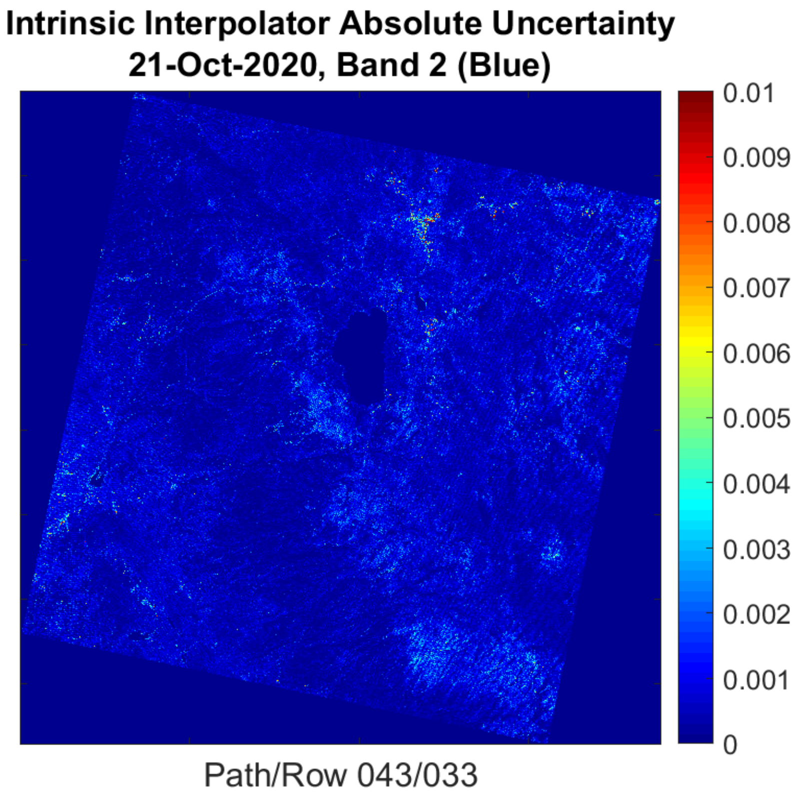

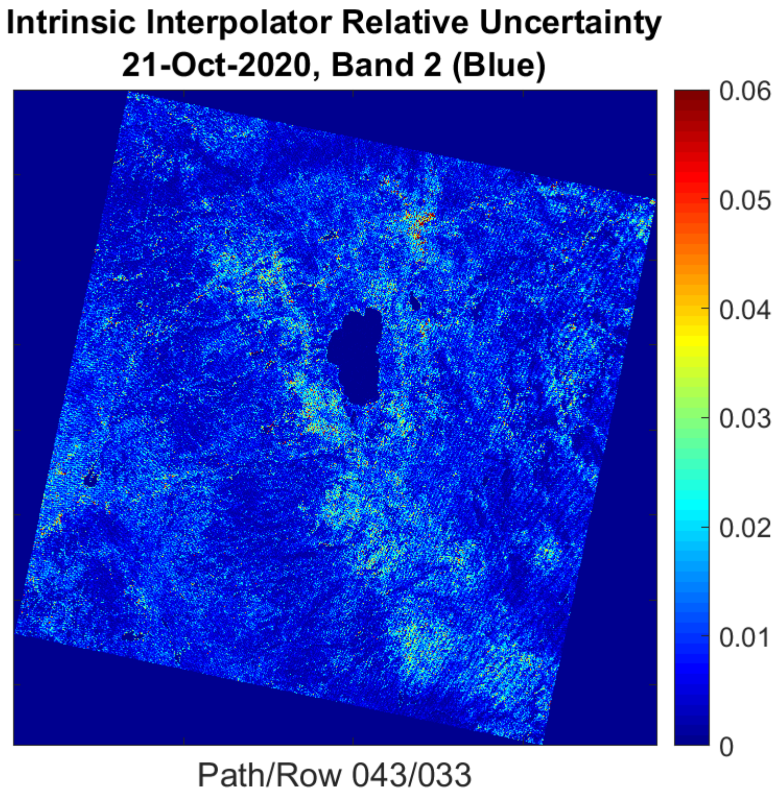

The water, where the data is very homogeneous, has very small intrinsic interpolation uncertainty. High contrast areas have more uncertainty. The fingerprint-like pattern in the uncertainty (accentuated by Matlab) is due to the offset between output and observation positions.

Intrinsic Interpolation Uncertainty - Reflectance

Lake Tahoe P43/R33
Red (Band 4)

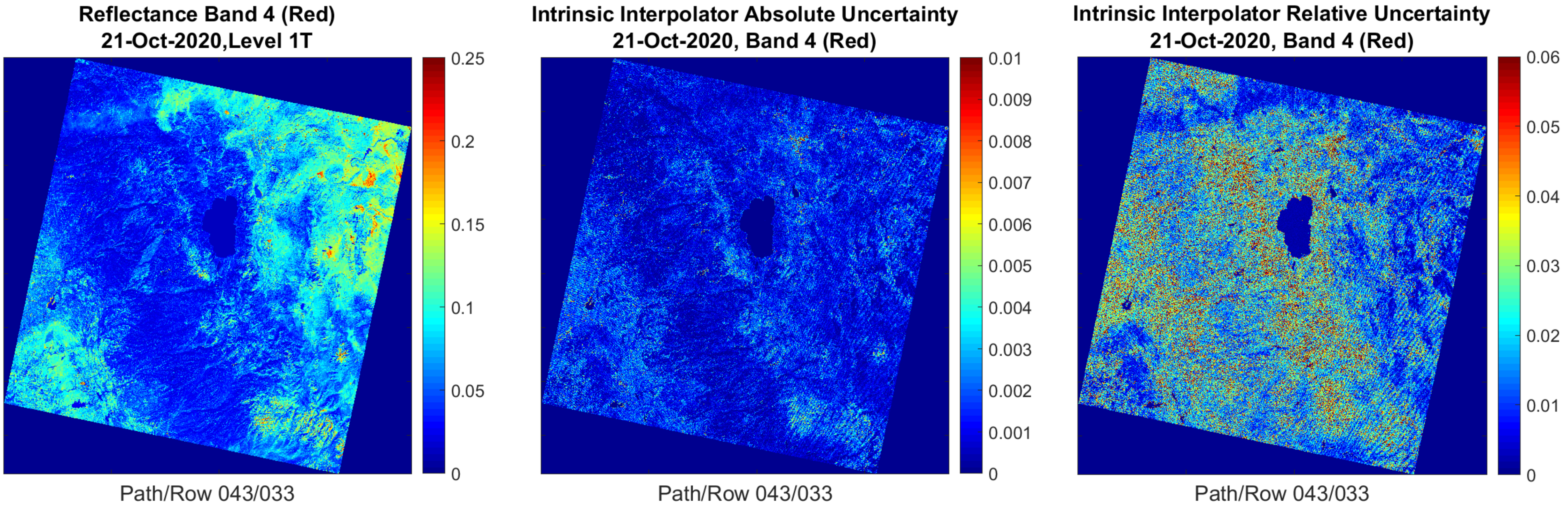

In the red band, there is a sharper contrast at the border of the lake, and this results is a higher intrinsic uncertainty.

Intrinsic Interpolation Uncertainty - Reflectance

Lake Pontchartrain P22/R39
Blue (Band 2)

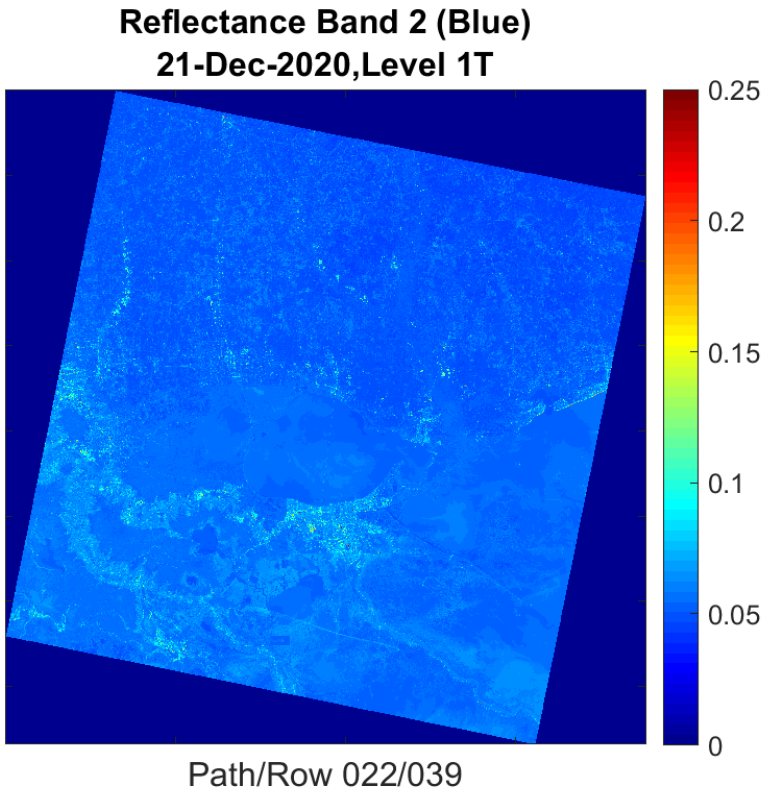

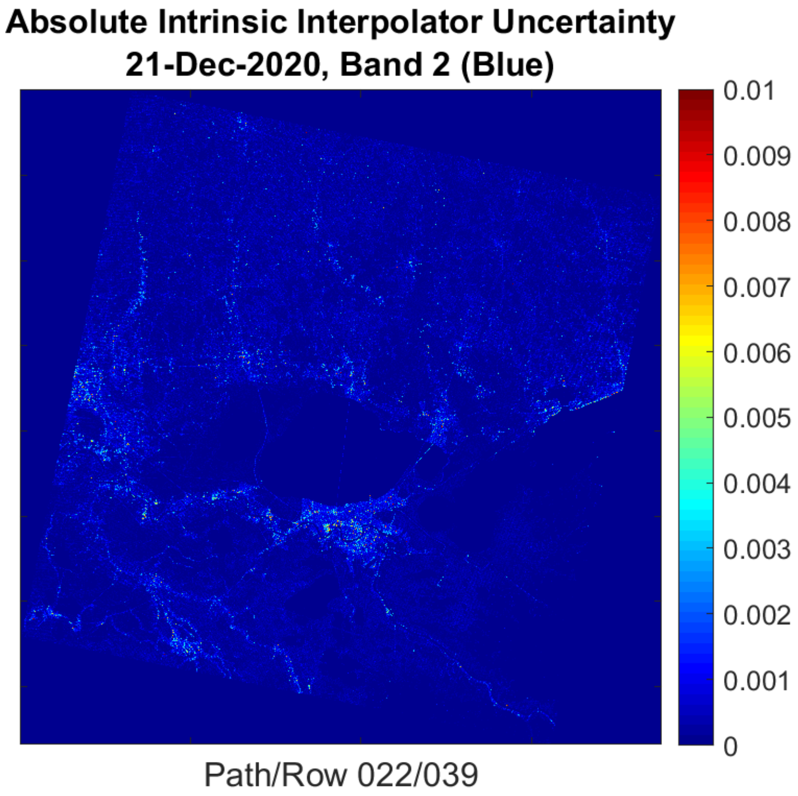

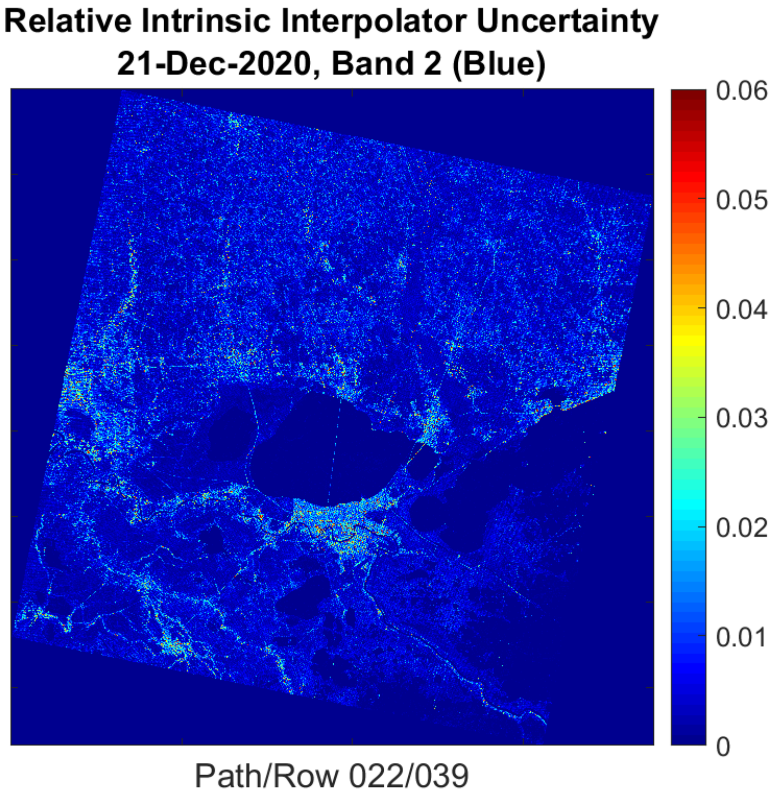

The water here again has low intrinsic uncertainty. The developed areas surrounding the lake have higher contrast and higher intrinsic interpolation uncertainty. The area on the southern border of the lake is New Orleans.

Intrinsic Interpolation Uncertainty - Reflectance

Lake Pontchartrain P22/R39
NIR (Band 5)

Reflectance Band 5 (NIR)
21-Dec-2020,Level 1T

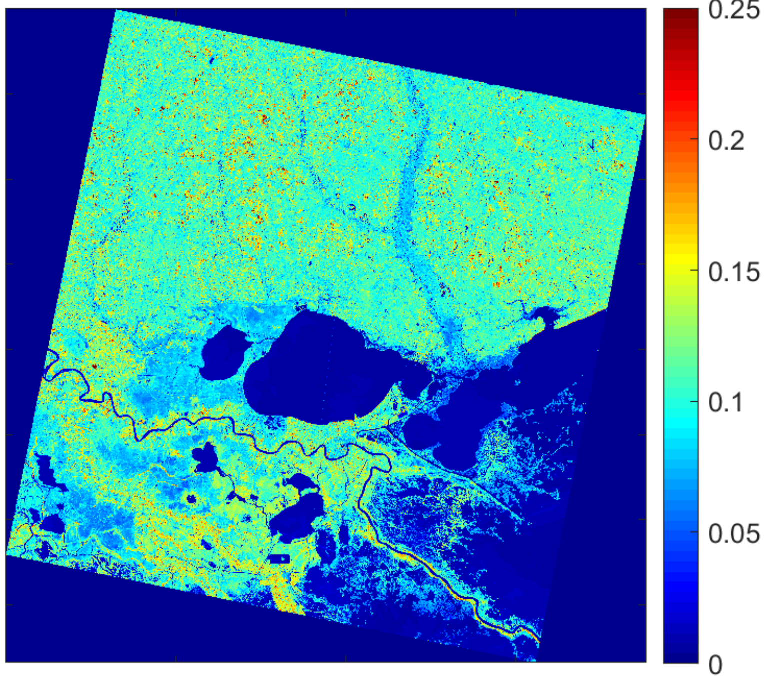

Path/Row 022/039

Absolute Intrinsic Interpolator Uncertainty
21-Dec-2020, Band 5 (NIR)

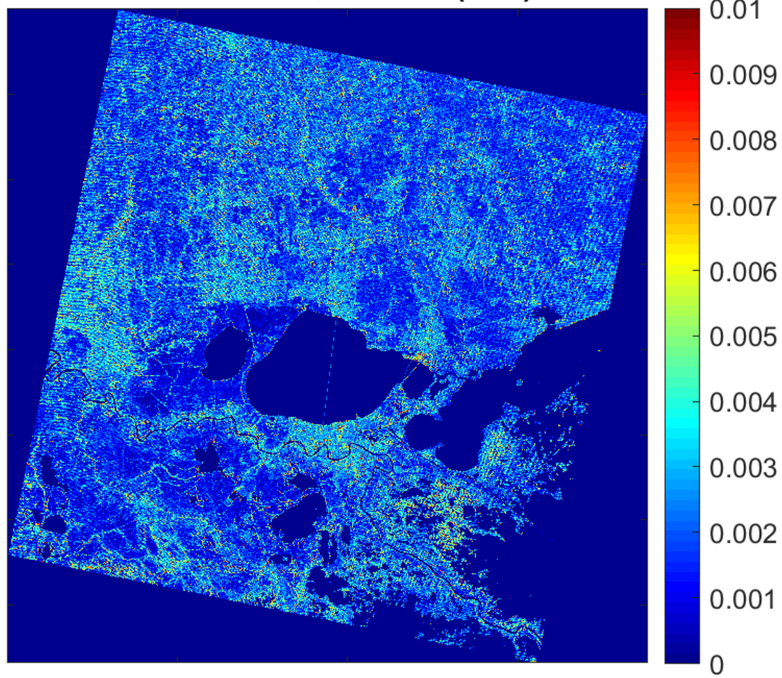

Path/Row 043/033

Relative Intrinsic Interpolator Uncertainty
21-Dec-2020, Band 5 (NIR)

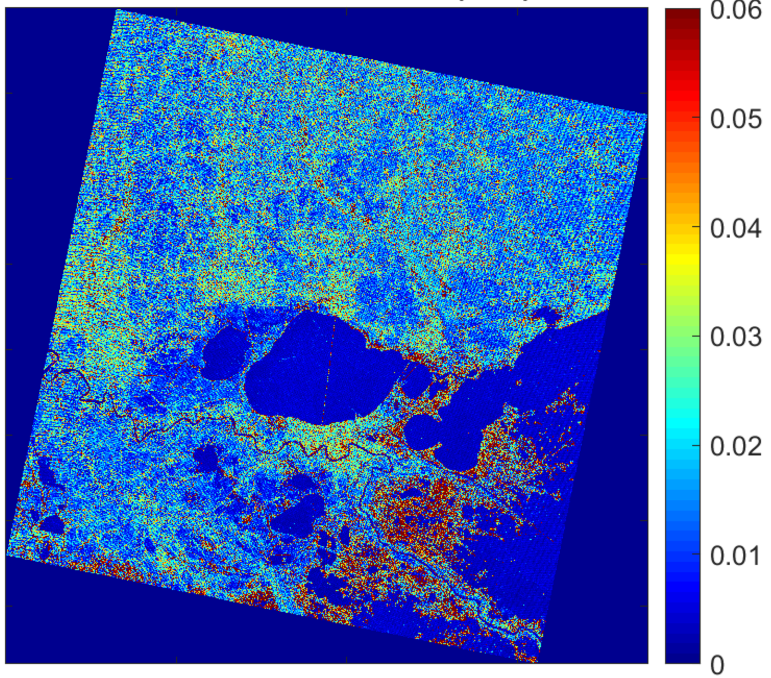

Path/Row 043/033

In the NIR band, the contrast can be seen in the uncertainty estimates. Notice the Lake Pontchartrain bridge crossing the center of the lake stands out in the uncertainty estimates.

Combining the Uncertainty Components

- **The combined uncertainty is the root sum of the squares of each component of the uncertainty**

$$\sigma_{total} = \sqrt{\sigma^2_{SI\ uncertainty} + \sigma^2_{noise} + \sigma^2_{intrinsic} + \sigma^2_{coupled}}$$

where, $\sigma_{SI\ uncertainty}$ = SI uncertainty
σ_{noise} = Resampled sensor noise
$\sigma_{intrinstic}$ = Intrinsic interpolation uncertainty
$\sigma_{coupled}$ = Coupled geometric and radiometric uncertainty

- **For pixels affected by saturation, this composite uncertainty is set to the unknown value**

Uncertainty Components

Lake Tahoe
P43/R33
Red Band

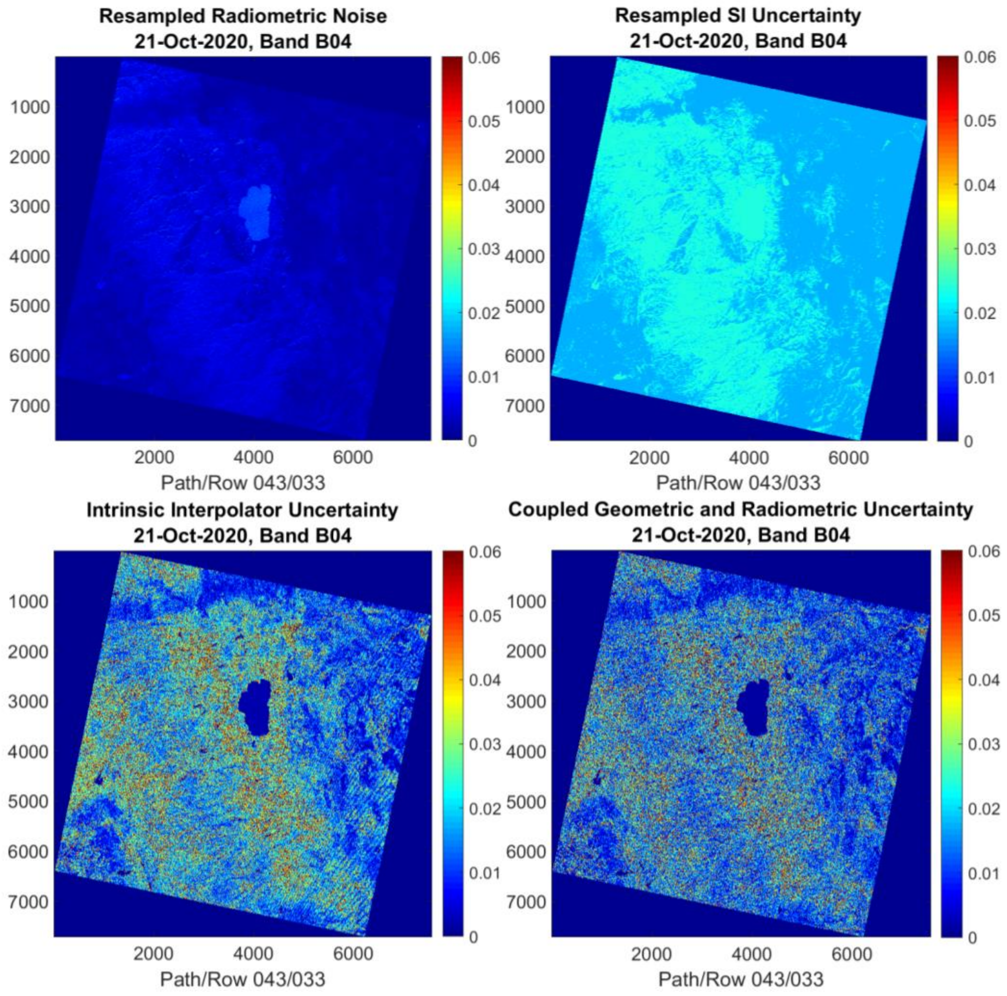

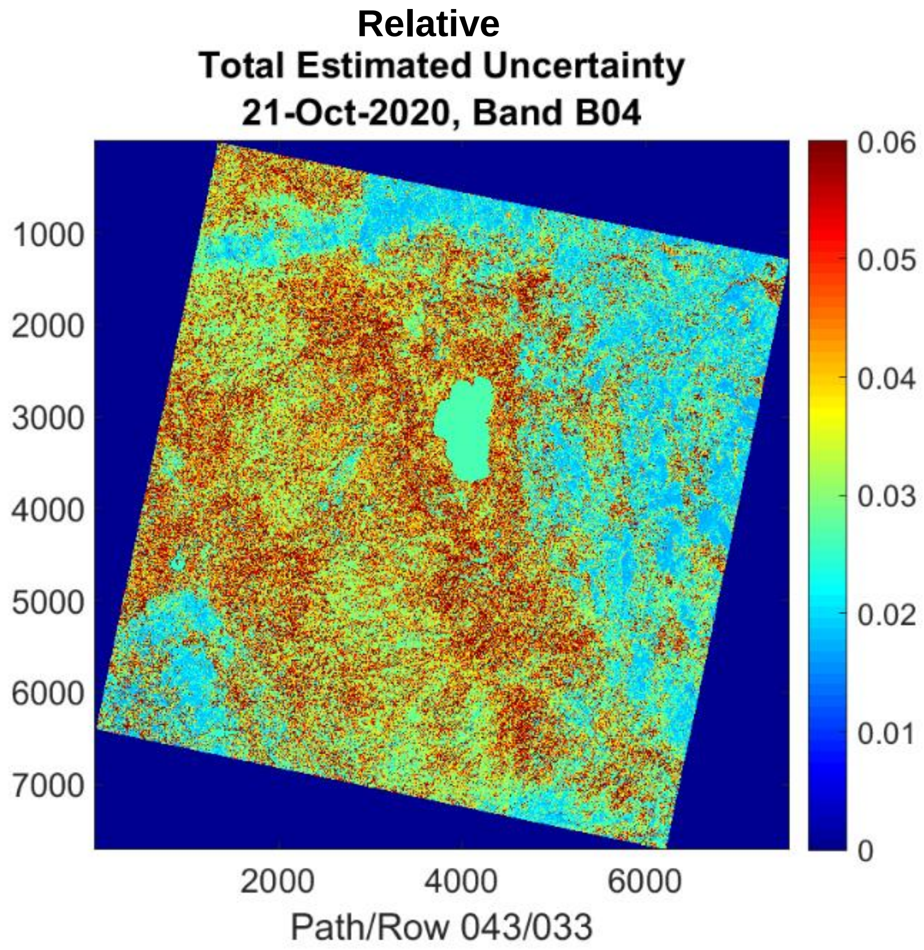

Uncertainty Component Histograms

Lake Tahoe
P43/R33
Red Band

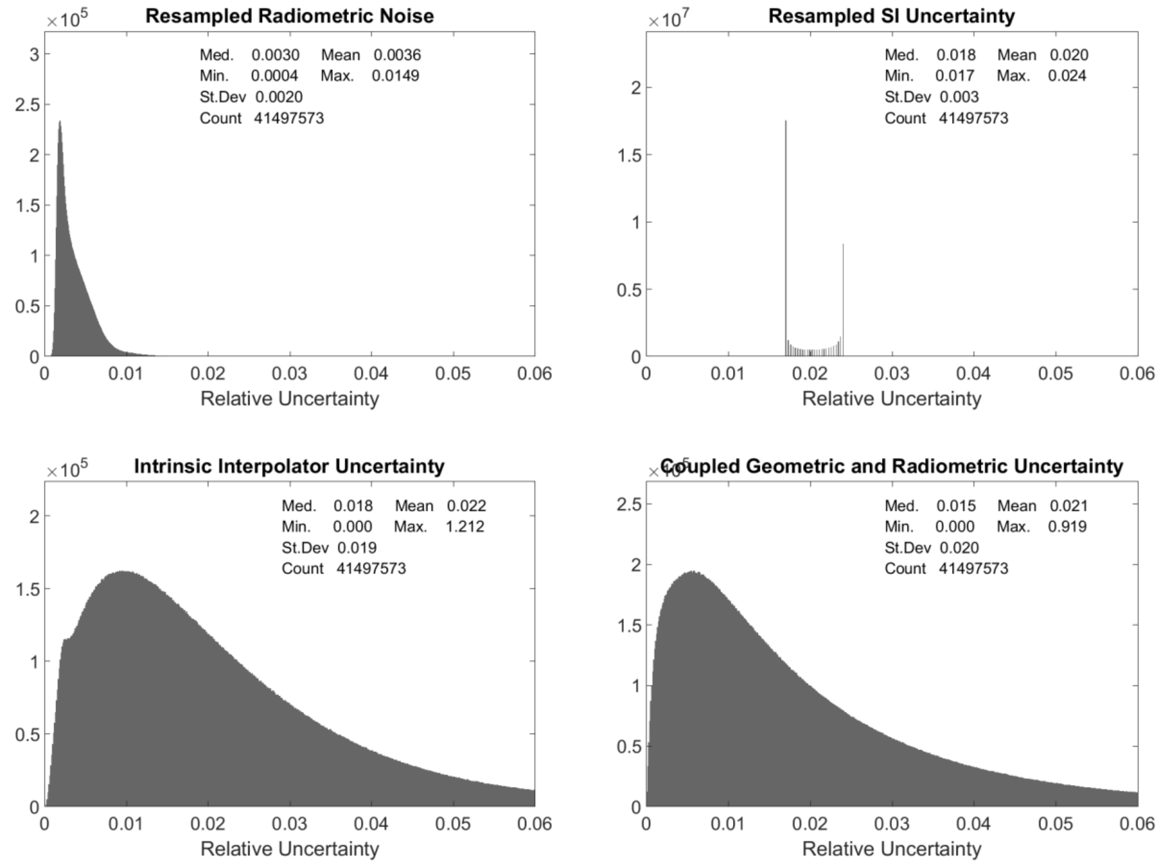

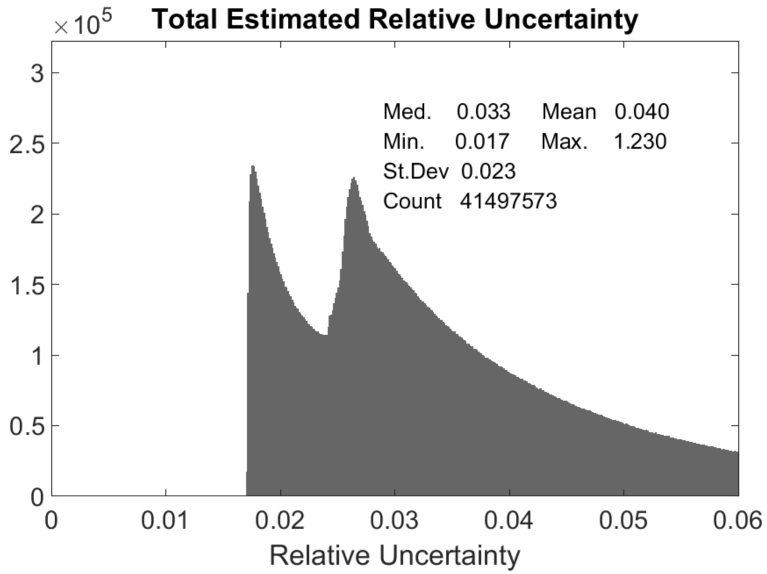

The double peak in the total uncertainty is a result of the SI uncertainty

Initial L2 Uncertainty Development

L2 Surface Reflectance Calculation

$$\rho_s = \frac{\rho_{TOA} - Tg_{OG}Tg_{O3}\rho'_{atm}}{Tg_{OG}Tg_{O3}Tr_{atm}\,Tg_{WV} + S_{atm}(\rho_{TOA} - Tg_{OG}Tg_{O3}\rho'_{atm})}$$

Inverted from Equation 1a in:

Vermote, Eric, Chris Justice, Martin Claverie, and Belen Franch. "Preliminary analysis of the performance of the Landsat 8/OLI land surface reflectance product." *Remote Sensing of Environment* 185 (2016): 46-56.

- **As implemented in LaSRC, several terms in the above equation are combined**
  - Tr_{atm} and Tg_{WV} are combined into a single term (Tt_{atmg})
  - $\rho'_{atm} = (\rho_{atm} - Xro_{rayp})\,Tg_{WVhalf} + Xro_{rayp}$
- **Uncertainty for many terms can be determined using input data uncertainty**
  - ρ_{toa}, Tg_{OG}, Tg_{O3}, Tg_{WV}, Tg_{WVhalf}, Xro_{rayp} are all interpolated using input ozone, water vapor and/or elevation values
- **Remaining terms do not have a straightforward uncertainty estimation**

L2 Algorithm Status

- **L2 Pixel Uncertainty algorithm still being defined**
  - Sensitivity analysis has been performed for several parameters
    - Used values directly calculated from input data to investigate the effect of water vapor and ozone transmission
  - Uncertainties will be estimated for individual terms in the surface reflectance equation
    - Using the LaSRC source code to identify inputs for each term
  - Estimating transmission uncertainty over a range of expected AOT, pressure, angle, water vapor and ozone values
    - Extending analysis to Rayleigh scattering (using cmg dem)
  - Identifying methods to define uncertainty for correlated terms

L1T GUI Implementation

GUI Overview

- **A graphical user interface (GUI) has been developed in MATLAB to allow the user to generate Landsat 8 L1T total or component uncertainty**
  - Each component can be computed individually
  - The user can also combine only the components of interest, or compute the composite of all of them
  - A compiled C-mex routine was created to compute the uncertainty components for which MATLAB itself would not be practical

Initial Landsat-8 L1 Pixel Uncertainty Tool

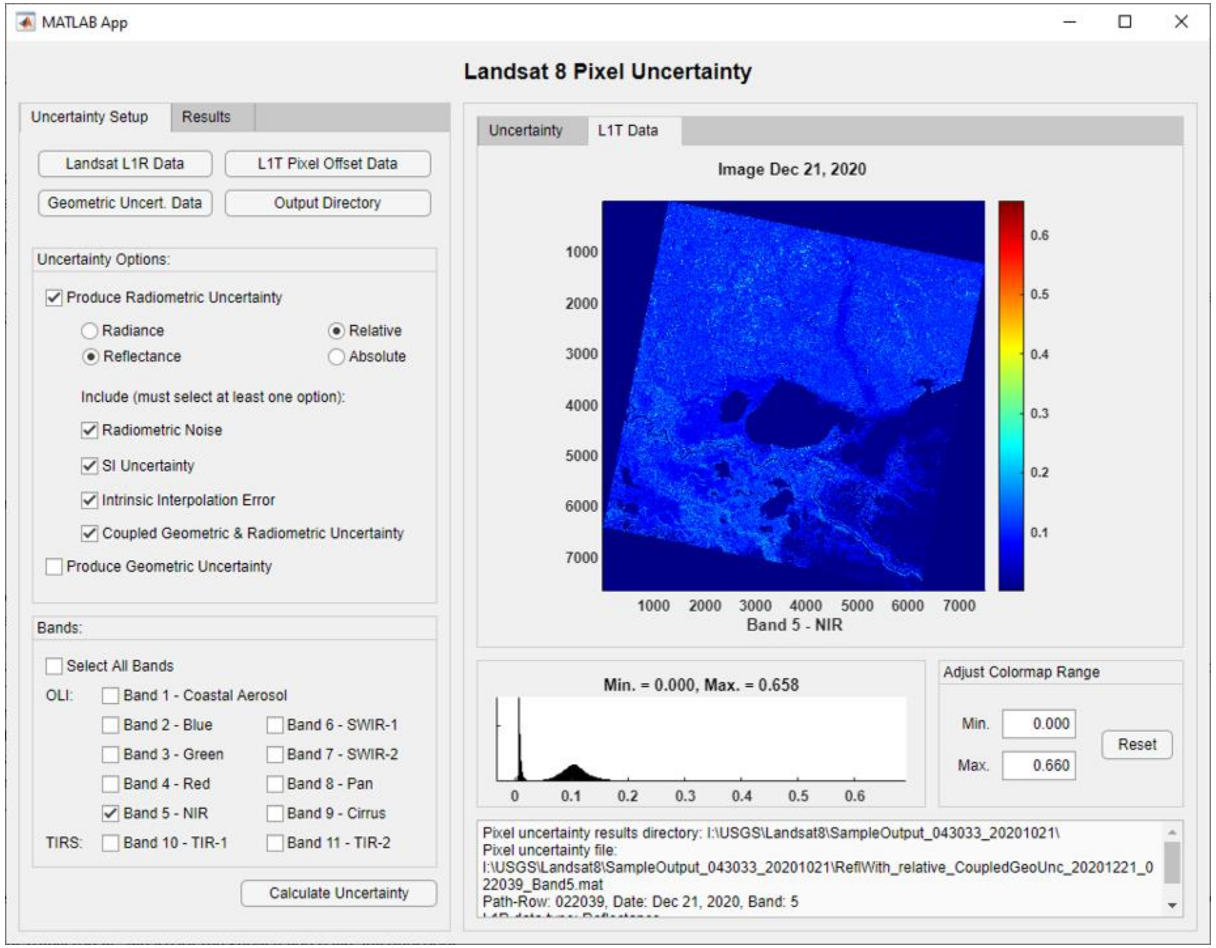

Initial Landsat-8 L1 Pixel Uncertainty Tool

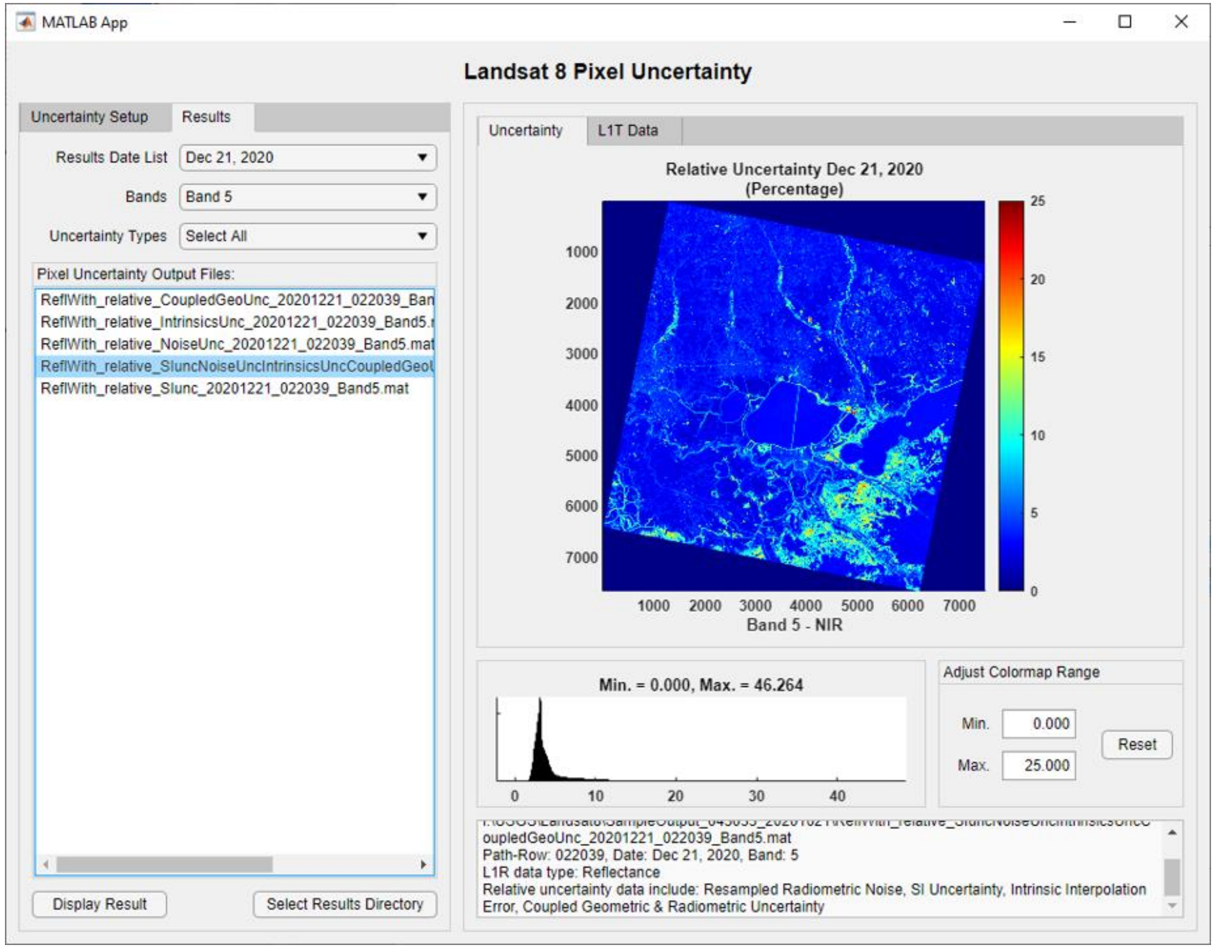

Special Thanks and Acknowledgements

- **This work has been funded by the USGS at the EROS Data Center under Subcontract SMS0004450 through Prime Contract Number 140G0121D0001 with KBR Services, LLC**

- **Technical contributions made by:**
  - Kara Burch, I2R
  - Obaidul Haque, KBR
  - Dr. Dennis Helder, SDSU/KBR
  - Esad Micijevic, USGS
  - Mary Pagnutti, I2R
  - Dr. Rajagopalan Rengarajan, KBR
  - Dr. Robert E. Ryan, I2R
  - Dr. David Sitton, I2R

Appendix

Intrinsic Interpolation Uncertainty Theoretical Background

- **Lagrange polynomial interpolation provides a cubic polynomial fitting 4 points**
  - Has a known error bound based on the 4^{th} derivative of the source, observation data
  - Matches the observations at 4 points
- **Akima and cubic convolution interpolators both use different cubic polynomials**
  - These are different than the cubic Lagrange interpolation polynomial
  - Match the data at 2 points and have derivatives based on the slopes between observation points
  - Often, these two interpolators are close to the Lagrange polynomial
    - Cubic convolution polynomial actual equals the Lagrange polynomial at the center of the region of interest
- **The Lagrange polynomial error can be extended to the other cubic interpolators**
  - The absolute difference between the Lagrange polynomial and the interpolated value is the same as the difference in their errors

Intrinsic Interpolation Uncertainty Theoretical Background

- **The uncertainty introduced by Lagrange polynomial interpolation is a function of the 4th derivative of the source**
  - The (oversampled) source is the convolution of the actual scene and the point spread function (PSF) of the sensor
  - Using convolution theory, the 4th derivative of the source data is the convolution of actual scene and the 4th derivative of the PSF
    - The actual scene can be estimated using the measured values (along with their uncertainties)
    - The PSF of the sensor can be found empirically using edge target measurements, or by assuming it is gaussian with measured FWHM
    - An upper bound is found for this convolution
- **The same method provides uncertainty estimates for both Landsat 8 interpolators**
  - Estimates using this technique are dependent on the distance from the edge of the interpolation region, and peak in the center of the region of interpolation

Mathematical Basis of Estimation

Error Estimate in terms of the 4th derivative of the source

- **Lagrange polynomial uncertainty estimate, for observations at points x_i and interpolation position x, where $x_1 < x_2 < x < x_3 < x_4$ and p_L is the Lagrange polynomial**

$$R_L(x) = f(x) - p_L(x) = \left(\frac{f^{(4)}(z_x)}{4!}\right)\prod_{i=1}^{4}(x - x_i) \quad \text{for some } z_x \in [x_1, x_4]$$

- **The error of the interpolation is bounded by this error plus the difference between the Lagrange polynomial and the interpolator, p_{int}**

$$|R_{int}(x)| \le |R_L(x)| + |p_L(x) - p_{int}(x)|$$

- **The observation positions and the polynomials here are known**
  - For cubic convolution interpolation, the values of x_i are $-1,0,1,2$
  - For Akima the values of x_i are the 4 center positions in the interpolation kernel
  - Need an upper bound on $f^{(4)}(z_x)$

Mathematical Basis of Estimation

Bounding the 4th Derivative

- **If S is the actual scene, and the sensor's point spread function is G, then the observations are the convolution of these**

$$f(x) = (S * G)(x)$$

- **The derivatives of f are can be written in terms of the source and derivative of G**

$$f'(x) = (S * G')(x)$$

$$f^{(4)}(x) = \left(S * G^{(4)}\right)(x)$$

- **Note that the source S is the sum of the observation (from the sensor) and an error term, and we already have an estimate of the distribution of this error**

$S = f(x) + \epsilon(x)$ **which can be rearranged to** $f(x) = S - \epsilon(x)$

- **The convolution of the source and the 4th derivative of the PSF can be bounded**

$$\left|f^{(4)}(x)\right| \approx \left|\left(S * G^{(4)}\right)(x)\right| \approx \left|\left(f * G^{(4)}\right)(x)\right| \leq (\max y_i) \int_{\{G^{(4)}(x)>0\}} G^{(4)}(x)dx - (\min y_i) \int_{\{G^{(4)}(x)\leq 0\}} \left|G^{(4)}(x)\right| dx$$

- **This gives a bound on the 4th derivative**
  - The integrals above are the same for all observations, and need only be calculated once

Cubic Convolution

Partial Derivatives

- **For the cubic convolution, the partial derivative with respect to x can be computed algebraically as follows**

$$x_i = x - (n-2) \quad \text{for } n = 1,2,3,4 \text{ and } x \in [0,1]$$

$$wgt(x_i) = \begin{cases} 3a|x_i|^2 - 10a\,x_i + 8a & \text{if } |x_i| < 1 \\ 3(a+2)|x_i|^2 - 2(a+3)|x_i| & 1 \le x_i \le 2 \\ 0 & \text{otherwise} \end{cases}$$

$$CubicConvolution(x, y_1, y_2, y_3, y_4) = \sum_i^4 wgt(x_i) y_i$$

$$\frac{\partial}{\partial y_i}\big(CubicConvolution(x, y_1, y_2, y_3, y_4)\big) = wgt(x_i)$$

$$u_{cc}^2 = \sum_{i=1}^4 \big(wgt(x_i)u(y_i)\big)^2$$

Modified Akima Interpolation

- **The modified Akima interpolator takes 6 input points(x_i , y_i) and the relative distance (z) of the interpolation point between the 3rd and 4th points,**

$dx_i = x_{i+1} - x_i$ $\quad$ $dy_i = y_{i+1} - y_i$ $\quad$ for $i = 1,2,\dots,5$

$m_i = \frac{dx_i}{dy_i}$ for $i = 1,2,\dots,5$ $\quad$ $s_i = |m_{i+1} - m_i|$ for $i = 1,2,3,4$

$$t_1 = \begin{cases} \dfrac{m_2 + m_3}{2} & if\ s_3 + s_1 = 0 \\ \dfrac{s_3 m_2 + s_1 m_3}{s_3 + s_1} & otherwise \end{cases} \qquad t_2 = \begin{cases} \dfrac{m_3 + m_4}{2} & if\ s_4 + s_2 = 0 \\ \dfrac{s_4 m_3 + s_2 m_4}{s_4 + s_2} & otherwise \end{cases}$$

The partial derivatives of the Akima interpolation are too complex to include here. To eliminate typographical errors, they were generated using MATLAB's Symbolic Toolbox and converted directly source code.

$$p_1 = y_3$$

$$p_2 = t_1$$

$$p_3 = \frac{3m_3 - 2t_1 - t_2}{dx_3}$$

$$p_4 = \frac{t_1 + t_2 - 2m_3}{dx_3^2}$$

For $0 \le z \le dx_3$

$$AkimaInterp(x_1, x_2, \dots, x_6, y_1, y_2, \dots, y_6, z) = p_1 + p_2 z + p_3 z^2 + p_4 z^3$$